Article:
Gao, W, Rigout, M orcid.org/0000-0002-4894-7768 and Owens, H (2017) Optical properties of cotton and nylon fabrics coated with silica photonic crystals. Optical Materials Express, 7 (2). 279207. pp. 341-353. ISSN 2159-3930

https://doi.org/10.1364/OME.7.000341

The optical properties of cotton and nylon fabrics coated with silica photonic crystals

WEIHONG GAO[1,2], MURIEL RIGOUT[3], AND HUW OWENS[2,*]

[1]*College of Fashion, Shanghai University of Engineering Science, Shanghai, 201620, China*
[2]*School of Materials, The University of Manchester, Manchester, M13 9PL, UK*
[3]*School of Design, University of Leeds, Leeds, LS2 9JT, UK*
**Huw.Owens@manchester.ac.uk*

Abstract: In this work, colourant-free coloured fabrics have been produced by the self-assembly of silica nanoparticles (SNPs) using a natural sedimentation method. The optical properties of the SNP-coated fabrics were investigated and the spectral reflectance, chromaticity coordinates, and CIE L* a* b* values are reported. The overall colour effect on the fabric can be described by Bragg's diffraction of the ordered SNP photonic crystal and the Mie scattering of the disordered SNP arrangement. It was found that the structural colour on the tight black woven cotton fabric was more uniform than that from the loose black knitted nylon fabric. Although the structural colour was not easily perceived on a white fabric due to the strong reflection of the white background, the SEM images show that an ordered photonic crystal was formed on the fabric and a small colour difference by the introduction of SNPs was measured using instrumental colour measurement.

OCIS codes: (160.6030) Silica; (050.5298) Photonic crystal; (160.4760) Optical properties; (330.1690) Color; (160.1245) Artificially engineered materials.

References and links

1. S. Kinoshita, *Structural colors in the realm of nature* (World Scientific, 2008).
2. J. Xu and Z. Guo, "Biomimetic photonic materials with tunable structural colors," J. Colloid Interface Sci. 406, 1–17 (2013).
3. F. Meseguer, "Colloidal crystals as photonic crystals," Colloids Surfaces A Physicochem. Eng. Asp. 270–271, 1–7 (2005).
4. P. J. Darragh, A. J. Gaskin, and J. V. Sanders, "Opals," Sci. Am. 234(4) 84–95 (1976).
5. R. J. D. Tilley, *Colour and the optical properties of materials* (John Wiley & Sons, Ltd, 2010).
6. F. Marlow, P. Sharifi, R. Brinkmann, and C. Mendive, "Opals: status and prospects," Angew. Chem. Int. Ed. Engl. 48(34), 6212–6233 (2009).
7. J. F. Galisteo-López, M. Ibisate, R. Sapienza, L. S. Froufe-Pérez, A. Blanco, and C. López, "Self-assembled photonic structures," Adv. Mater. 23(1), 30–69 (2011).
8. Z. Li, J. Wang, and Y. Song, "Self-assembly of latex particles for colloidal crystals," Particuology 9(6), 559–565 (2011).
9. D. J. Norris, E. G. Arlinghaus, L. Meng, R. Heiny, and L. E. Scriven, "Opaline Photonic Crystals: How Does Self-Assembly Work?," Adv. Mater. 16(16), 1393–1399 (2004).
10. R. Mayoral, J. Requena, J. S. Moya, C. López, A. Cintas, H. Miguez, F. Meseguer, L. Vázquez, M. Holgado, and Á. Blanco, "3D Long-range ordering in an SiO2 submicrometer-sphere sintered superstructure," Adv. Mater. 9(3), 257–260 (1997).
11. P. Jiang and J. Bertone, "Single-crystal colloidal multilayers of controlled thickness," Chem. Mater. 11, 2132–2140 (1999).
12. S. H. Park, D. Qin, and Y. Xia, "Crystallization of mesoscale particles over large areas," Adv. Mater. 10(13) 1028–1032 (1998).
13. P. Jiang and M. J. McFarland, "Large-scale fabrication of wafer-size colloidal crystals, macroporous polymers and nanocomposites by spin-coating," J. Am. Chem. Soc. 126(42), 13778–13786 (2004).
14. J. Park and J. Moon, "Control of colloidal particle deposit patterns within picoliter droplets ejected by ink-jet printing," Langmuir 22(8), 3506–3513 (2006).
15. B. Cheng, P. Ni, C. Jin, Z. Li, D. Zhang, P. Dong, and X. Guo, "More direct evidence of the fcc arrangement for artificial opal," Opt. Commun. 170, 41–46 (1999).
16. X. Sun, J. Zhang, X. Lu, X. Fang, and H. Peng, "Mechanochromic photonic-crystal fibers based on continuous sheets of aligned carbon nanotubes," Angew. Chem. Int. Ed. Engl. 54(12), 3630–3634 (2015).
17. J. Zhang, S. He, L. Liu, G. Guan, X. Lu, X. Sun, and H. Peng, "The continuous fabrication of mechanochromic fibers," J. Mater. Chem. C 4, (2016).

18. N. Zhou, A. Zhang, L. Shi, and K.-Q. Zhang, "Fabrication of Structurally-Colored Fibers with Axial Core–Shell Structure via Electrophoretic Deposition and Their Optical Properties," ACS Macro Lett. 2(2), 116–120 (2013).
19. Z. Liu, Q. Zhang, H. Wang, and Y. Li, "Structural colored fiber fabricated by a facile colloid self-assembly method in micro-space," Chem. Commun. 47, 12801–12803 (2011).
20. G. Liu, L. Zhou, Q. Fan, L. Chai, and J. Shao, "The vertical deposition self-assembly process and the formation mechanism of poly(styrene-co-methacrylic acid) photonic crystals on polyester fabrics," J. Mater. Sci. 51(6), 2859–2868 (2016).
21. G. Liu, L. Zhou, Y. Wu, C. Wang, Q. Fan, and J. Shao, "The fabrication of full color P(St-MAA) photonic crystal structure on polyester fabrics by vertical deposition self-assembly," J. Appl. Polym. Sci. 132, 41750–41759 (2015).
22. J. Shao, Y. Zhang, G. Fu, L. Zhou, and Q. Fan, "Preparation of monodispersed polystyrene microspheres and self-assembly of photonic crystals for structural colors on polyester fabrics," J. Text. Inst. 105(9), 938–943 (2014).
23. Y. Y. Diao, X. Y. Liu, G. W. Toh, L. Shi, and J. Zi, "Multiple structural coloring of silk-fibroin photonic crystals and humidity-responsive color sensing," Adv. Funct. Mater. 23, 5373–5380 (2013).
24. Y. Y. Diao and X. Y. Liu, "Bring Structural Color to Silk Fabrics," Advanced Materials Research 441, 183–186 (2012).
25. G. Liu, L. Zhou, Y. Wu, C. Wang, Q. Fan, and J. Shao, "Optical properties of three-dimensional P(St-MAA) photonic crystals on polyester fabrics," Opt. Mater. 42, 72–79 (2015).
26. L. Zhou, Y. Wu, G. Liu, Y. Li, Q. Fan, and J. Shao, "Fabrication of high-quality silica photonic crystals on polyester fabrics by gravitational sedimentation self-assembly," Color. Technol. 131(6), 413–423 (2015).
27. L. Zhou, G. Liu, Y. Wu, Q. Fan, and J. Shao, "The synthesis of core-shell monodisperse P(St-MAA) microspheres and fabrication of photonic crystals Structure with Tunable Colors on polyester fabrics," Fibers Polym. 15(6), 1112–1122 (2014).
28. L. Zhou, Y. Li, G. Liu, Q. Fan, and J. Shao, "Study on the correlations between the structural colors of photonic crystals and the base colors of textile fabric substrates," Dye. Pigment. 133, 435–444 (2016).
29. W. Gao, M. Rigout, and H. Owens, "Facile control of silica nanoparticles by a novel solvent varying method for the fabrication of artificial opal photonic crystals," J. Nanoparticle Res. (to be published).
30. W. Stöber, A. Fink, and E. Bohn, "Controlled growth of monodisperse silica spheres in the micron size range," J. Colloid Interface Sci. 26(1), 62–69 (1968).
31. ISO 105-B02:2014 Textiles — Tests for colour fastness — Part B02: Colour fastness to artificial light: Xenon arc fading lamp test.
32. L. Shi, Y. Zhang, B. Dong, T. Zhan, X. Liu, and J. Zi, "Amorphous photonic crystals with only short-range order," Adv. Mater. 25(37), 5314–5320 (2013).
33. W. Gao, M. Rigout, and H. Owens, "Self-assembly of silica colloidal crystal thin films with tuneable structural colours over a wide visible spectrum," Appl. Surf. Sci. 380, 12–15 (2016).
34. B. N. Khlebtsov, V. A. Khanadeev, and N. G. Khlebtsov, "Determination of the size, concentration, and refractive index of silica nanoparticles from turbidity spectra," Langmuir 24(16), 8964–70 (2008).
35. E. Marx and G. W. Mulholland, "Size and Refractive Index Determination of Single Polystyrene Spheres," J. Res. Natl. Bur. Stand," 88(5), 321-338 (1983).
36. H. Franke, H. G. Festl, and E. Krätzig, "Light induced refractive index changes in PMMA films doped with styrene," Colloid Polym. Sci. 262(3), 213–216 (1984).
37. W. Yuan, N. Zhou, L. Shi, and K.-Q. Zhang, "Structural Coloration of Colloidal Fiber by Photonic Band Gap and Resonant Mie Scattering," ACS Appl. Mater. Interfaces 7(25), 14064–14071 (2015).
38. R. McDonald, *Colour Physics for Industry* (Society of Dyers and Colourists, 1997).

1. Introduction

Colour caused by the physical structure of a material, rather than dye or pigment molecules, is generally referred to as 'structural colour' [1]. Photonic crystals (PCs) with a periodic three-dimensional nanostructured system are such materials showing structure colours [2]. If the periodic nanomaterial is self-assembled from colloidal spheres, such as silica or polystyrene (PS), the system is known as a colloidal crystal (CC) or colloidal PC (CPC) [3]. Natural precious opals consisting of highly ordered silica nanoparticles (SNPs) are probably the oldest and best-known example of PCs with tuneable structural colours [4]. The reflection properties of these opals have been explained using a modified version of Bragg's diffraction theory [5].

Inspired by natural opals, scientists have successfully fabricated artificial opal PCs using bottom-up self-assembly techniques [6]–[9], such as natural sedimentation [10], vertical

deposition [11], physical confinement [12], spinning coating [13], and ink-jet printing [14]. The self-assembled artificial opal has a close-packed face-centred-cubic crystal structure, which contributes to Bragg's diffraction of white light and results in structural colours. The quality of the structural colour produced mainly depends on the uniformity of the spheres and the regularity of the crystal structure [15]. In most studies, the adopted substrate for the self-assembly of the SNPs is smooth and flat, such as a glass surface or silicon wafer, as this helps to produce a long-range ordered PC and high-quality structural colour.

In recent years, there has been a growing interest in fabricating PCs on flexible textile fibres [16]–[19] and fabrics [20]–[26] to achieve structural colouration due to the straightforward control of colours by sphere size and the possibility of replacing chemical dyes and pigments with environmental friendly polymer or silica spheres. However, the research in this emerging area has focused on the self-assembly of PS based colloids on a smooth textile substrate such as silk and polyester. This is probably because the PS size can be easily controlled by using a soap-free emulsion polymerization technique and the smoother surface can improve the quality of the PC and structural colours. For example, Diao *et al.* [23], [24] have successfully produced silk fabrics with red and yellow/green structural colours by the natural sedimentation of 270 nm- and 240 nm-sized PS spheres. Using the same technique and spheres, Shao *et al.* [22] fabricated red, yellow, and cyan coloured polyester fabrics by using PS spheres with diameters of 270 nm, 240 nm, and 200 nm, respectively; this group has also self-assembled poly(styrene-methacrylic acid) spheres [25][27] or silica spheres [26] onto black woven polyester fabrics and produced a wider range of structural colours.

It should be noted that in the reported work, the textile substrates are completely covered with long-range CPCs, thus showing iridescent (angle-dependent) colour effects, which is not ideal for replacing conventional dyes or pigments. In addition, the use of a rough cotton substrate and knitted structure for the structural colouration has been rarely reported, and there is no systematic study of how the factors of fabric structure and fabric colour relate to the optical properties of the structurally coloured textile materials, although its been claimed that a black coloured fabric has a higher ability to absorb the incident light and enhance the chroma of the structural colour than a white coloured fabric [25][28].

In this paper, silica PCs have been self-assembled on different types of textile fabrics using the technique of natural sedimentation. The self-assembly behaviour of the SNP on the fabric was examined using SEM micrograph analysis. The effect of particle size, fabric structure (woven and knitted), and fabric colours (black and white) to the optical properties of the SNP-coated fabrics are discussed. This work reports the realisation of non-iridescent structural colours on flexible textile fabrics using silica spheres and it is the first study to show how fabric structure and background colour can affect the perceived structural colour.

2. Experimental

2.1 Chemicals and materials

The chemical reagents used throughout the experiments are displayed as follows: the precursor alkoxide tetraethyl orthosilicate (TEOS) (99.0%) was purchased from Sigma-Aldrich Co., LLC; the catalyst ammonia (NH_3, 25% in H_2O) and the solvent ethanol (EtOH, 99.9%) were obtained from Fisher Scientific Co., Ltd., UK; the hydrolyzing agent distilled water (DW) (H_2O, distilled by a USF-ELGA water purifier) was dispensed in the laboratory. All the chemicals were used as received without any further purification. Black woven cotton (BWC) fabrics (0.034g/cm^2), black knitted nylon (BKN) fabrics (0.016g/cm^2), and white knitted cotton (WKC) fabrics (0.022g/cm^2) were obtained directly from the dye house in the School of Materials at The University of Manchester, and they were used without any modification. The fabrics were cut into circular shapes with the same diameter of 25 mm. Specimen tubes were used for the colloidal SNPs to settle. A Gallenkamp brand hot-box laboratory oven was used to provide an elevated temperature in order to accelerate the colloidal self-assembly process.

2.2 Synthesis of uniform SNPs

Colloidal suspensions containing uniform SNPs were prepared using a modified Stöber-based solvent varying (SV) method as described in our previous work [29], [30], where hydrolysis and condensation of silicone alkoxide was catalyzed by ammonia. In a typical procedure, a starting mixture solution containing 8ml of ammonia, 47 ml of ethanol, and 3 ml of DW was prepared in a 250 ml round-bottom flask under vigorous stirring. When the temperature of the mixture solution reached 60 ºC, the TEOS (6 ml) was then added into the solution. The solution was stirred using an overhead motor with a PTFE stirrer blade for 2 h until the reaction completed. By fixing the volume of TEOS / H_2O / NH_3 (25%) and varying the volume of solvent EtOH (47 – 73 ml), uniform SNPs can be achieved in a controlled size range.

2.3 Sedimentation self-assembly of SNPs on fabrics

Textile fabrics of different constructions and background colours were successfully coated with silica photonic crystals by the gravity sedimentation self-assembly of uniform SNPs. Using black woven cotton fabric as an example, a small circular piece of fabric ($\pi \times 25 \times 25$ mm^2) was placed on the bottom of a specimen tube, and then 3 ml of silica suspension without any purification and/or modification was poured into the tube to cover the fabric. The specimen tube was carefully transferred into an oven with an isothermal temperature of 60 ºC. The self-assembly and crystallization rate of the SNPs was accelerated with the use of an elevated temperature. Finally, as the solvent evaporated, SNPs were deposited onto the surface of the fabric due to gravity force. Using this surface coating of uniform SNPs, structurally coloured cotton fabric was produced due to the ordered silica PC formed on the surface of the black fabric. A wide range of structural colours was obtained on the black woven cotton fabrics by applying silica suspensions containing different sized SNPs, Fig. 1a-e. The black knitted nylon and white knitted cotton were treated with the same silica batches and using the same self-assembly conditions.

2.4 Characterisation of SNPs and SNP-coated fabrics

To determine the morphological properties of the SNPs, SNP-coated fabrics were examined using a Hitachi S-3000N scanning electron microscopy (SEM). The particle diameter and particle size distribution of the SNPs was determined using a Malvern Zetasizer Nano S dynamic light scattering (DLS) device. An image of the SNP-coated fabrics was captured using the digital camera of an iPhone 5s. The spectral reflectance and chromaticity coordinates of the fabric samples were measured using a Datacolor 650 spectrophotometer. The colourfastness to light was tested (ISO 105-B02:2014 [31]) by exposing the samples to artificial daylight produced by a Xenon Light Fastness Tester (James Heal Co., Ltd.).

3. Results and discussion

In this work, photonic crystals have been successfully applied to textile fabrics through the self-assembly of SNPs. The SNP-coated fabrics were all graded 8 using the blue wool scale, indicating the excellent light fastness of the SNP-coated fabrics. The optical properties of the SNP-coated fabrics were affected by several factors such as the SNP diameter, fabric structure, and fabric background colour.

3.1 Effect of particle size on the structural colour of SNP-coated fabrics

Due to the uniformity of the SNPs and the controlled sedimentation conditions, photonic crystal structures can be self-assembled on the surface of the fabric. The fabric shows structural colours following Bragg's diffraction of white light incident on the silica photonic crystals. In addition, the structural colour can be tuned by varying the particle size of the SNP so that a wide range of visible spectral colours from red to blue could be achieved.

Fig. 1(a)-(e) shows the structurally coloured BWC fabrics that were produced from the coating of SNPs with different sized diameters. In general, the fabrics show monochromatic and uniform structural colours, and the colour was SNP size-dependent and non-iridescent (see **Visualization 1**). The surface SEM images of the fabric samples in Fig. 1(a) are given in Fig. 1(f)-(i) at different magnifications. At the lower magnification of 25 times, Fig. 1(f), the tight woven structure of the cotton fabric, and the smooth SNP fragments can be observed. Fig. 1(g) shows the particle arrangement of the fragments, which indicates a typical face-centred-cubic (fcc) photonic crystal structure. A particular structural colour will be produced by the diffraction from the ordered fcc crystal structure. However, in some areas, due to the uneven surface of the fabric the SNP coating is not continuous, some cracks as well as disordered particle arrangement are formed, as shown in Fig. 1(h), this affects the quality of the crystal and hence the structural colour produced. For example, in Fig. 1(i), the fibre is not completely covered by the spheres and the spheres are randomly distributed, so an opalescent colour from the Mie scattering of the white silica particles or dark colour from the light absorption with the original black fibre will be produced. It should be noted that these localised defects resulted in a short-range order [32] of the photonic crystals, producing structural colours with non-iridescent (angle-independent) effects, the essential requirement for real dyes and pigments.

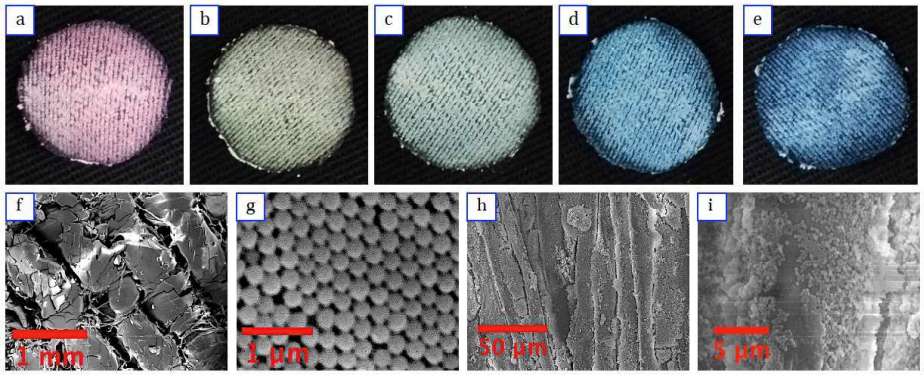

Fig. 1. Images of BWC fabrics coated with SNPs having average diameters of 342 nm, 287 nm, 262 nm, 233 nm, and 204 nm, from (a) to (e), respectively; the surface SEM images of (a) are given at the different magnifications of 25 (f), 20K (g), 400 (h), and 5K (i), the scale bars are added for these SEM images. The fabric diameter is 25 mm. **Visualization 1** shows images of the fabric samples from 0 to 60 degrees at 15 degree intervals.

The spectral reflectance of the structurally coloured BWC fabrics is given in Fig. 2(a), where it can be seen that the peak wavelength shifts systematically with particle size. Specifically, when the SNP diameter decreases from 342 nm, 287 nm, 262 nm, 233 nm, to 204 nm, the peak wavelengths of the structural colours have a blue-shift from 610 nm, 560 nm, 500 nm, 440 nm, to 390 nm, respectively. In addition, the distribution of wavelengths around the peak wavelength of the 262 nm-coated fabric (the green line in Fig. 2(a)) are broader than those of the other fabrics. Therefore, the green fabric in Fig. 1(c) looks duller (less chroma) than the other fabrics. This may be due to the slightly larger PDI value for the 262nm batch of SNPs. These peak wavelengths (y axis) are plotted against the particle diameters (x axis) as shown in Fig. 2(b), which are marked as diamond shapes. In comparison, the data determined experimentally by Zhou *et al.* [26], Liu *et al.* [25], and Diao *et al.* [24] was plotted based on SNP-coated polyester (square markers), P(St-MMA)-coated polyester (triangle markers), and PS-coated silk (circular markers), respectively. A best-fit linear trend line for the data is added, the linear function of the trend line and correlation coefficient R^2 values are given in Fig. 2(b).

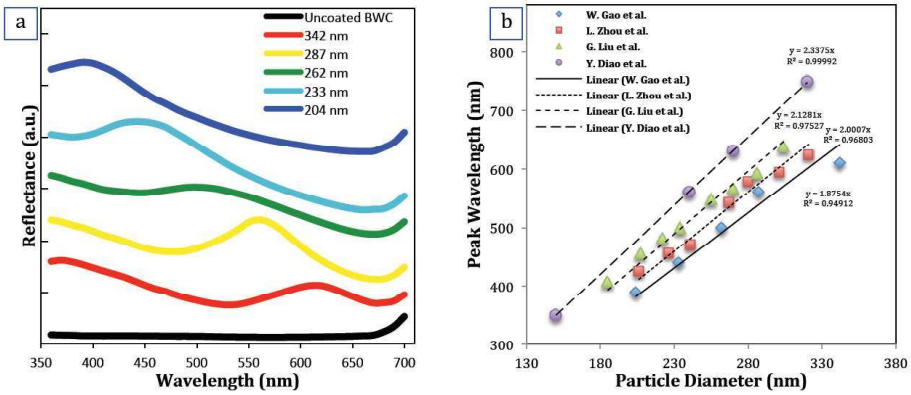

Fig. 2. Normalised reflectance spectra (a) of the original BWC fabric and the fabric coated with SNPs having average diameters given in the figure legend; plot of the peak wavelength (b) of SNP-coated cotton, SNP-coated polyester, P(St-MMA)-coated polyester, and PS-coated silk fabrics against the average particle diameter, data obtained from Fig. 2(a), Zhou *et al.* [26], Liu *et al.* [25], and Diao *et al.* [24], respectively; a linear trend line for each set is added with the linear function and correlation coefficient R^2 values presented.

It is known that the peak wavelength of a PC can be predicted using a modified Bragg's equation [5][33]:

$$\lambda = 1.633 n_{eff}\, d, \tag{1}$$

where λ is the peak wavelength of the material, d is the particle diameter, n_{eff} is the effective refractive index (RI) of the material. According to Eq. (1), the slope of the function in Fig. 2 equals $1.633 n_{eff}$, so the n_{eff} is calculated as 1.15, 1.23, 1.30, and 1.43 for the SNP-coated cotton, SNP-coated polyester, PS(St-MMA)-coated polyester, and PS-coated silk, respectively. If the spheres completely cover the fabric's surface, the effective RI of the fabric will depend on the RI of the sphere coating. It is known that the RI of silica spheres (1.475) [34] is smaller than PS (1.615) [35] and PS(St-MMA) spheres (1.511-1.515) [36], so the silica-coated fabric has a lower effective RI than PS or P(St-MMA)-coated fabrics. As for the silica-coated fabrics, the cotton has a lower RI than polyester and silk, so the effective RI of the SNP-coated cotton measured in our work is the smallest among all of the reported fabrics.

Generally, the smoother and flatter the substrate, the more likely an ordered high-quality PC will form on its surface. Therefore, a photonic crystal produced on polyester and silk is more ordered and continuous than one produced on cotton because the polyester and silk materials have smoother and flatter surfaces than cotton. This is demonstrated by the reducing R^2 values from 0.99992 to 0.94912, as shown in Fig. 2(b). However, the long-range ordered high-quality PCs will lead to iridescent (angle-dependent) structural colours [33], which is less desirable than the non-iridescent colours produced in this work for textile applications.

3.2 Effect of fabric structure on the optical properties of SNP-coated fabrics

The self-assembly of SNPs on woven-structured fabrics has produced uniform, SNP size-dependent, and non-iridescent structural colours; Fig. 1. In addition, such structural colours were also produced on the knitted-structured fabric. Fig. 3(a)-(e) shows the structurally coloured BKN fabrics prepared by the coating of SNPs with average diameters ranging from 342 nm to 204 nm. It can be seen that the structural colour produced on the knitted fabrics is also SNP size-dependent and they show similar hue properties compared with the BWC fabric coated with the same SNP size. However, these structural colours are less uniform because some of the surface is poorly covered by SNPs, therefore showing large areas of dark colour from the original black fabrics. The reason for the colour difference is probably from the loose knitted structure. Under the same self-assembly conductions, there are greater numbers of SNPs passing through the yarn spacing of the knitted structure than one of the woven

structure. In addition, the flexible knitted loop is likely to expand when drying the SNP suspension at a temperature of 60 ^{o}C, this facilitates the penetration of the SNPs into the fabric.

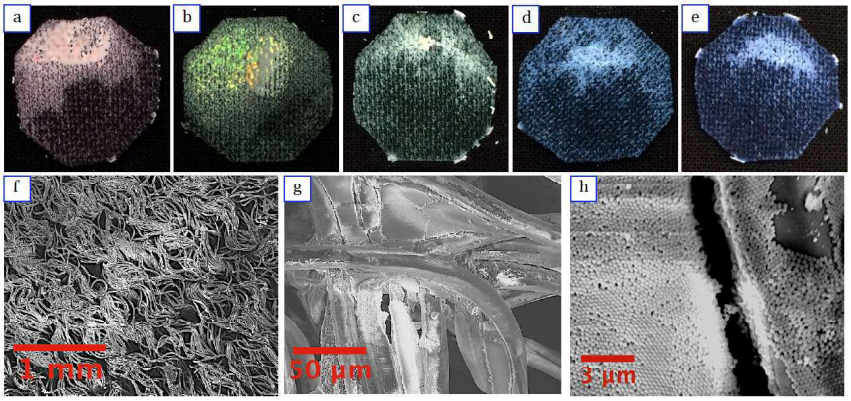

Fig. 3. Images of the BKN fabrics coated with SNPs having average diameters of 342 nm, 287 nm, 262 nm, 233 nm, and 204 nm, from (a) to (e), respectively; the surface SEM images of (b) are given at different magnifications of 25 (f), 400 (g), and 5K (h). The fabric diameter is approximately 25 mm.

In Fig. 3(f), it can be seen that the SNPs did not cover the whole fabric's surface, as the individual nylon fibres and the spacing between them are clearly observed. Fig. 1(g) shows a closer observation of the fabric surface, where you can see the SNP self-assembly behaviour. SNPs in the form of smooth fragments and disordered aggregations are found in-between the fibres. The hue of the structural colour is mainly from the smooth fragment area, where SNPs are self-assembled into the photonic crystal structure with an fcc arrangement as shown on the left side of Fig. 3(h). The white opalescent colour in Fig. 3(a)-(e) is from the disordered SNP aggregation or thin layer of SNP coating on the fibre surface as shown in the right side of Fig. 3(h), while the uncovered fibre surface area resulted in a dark colour due to the black background of the original fabric.

To investigate the effect of fabric structure on the optical properties of the SNP-coated fabric, the comparisons of the spectral reflectance and chromaticity coordinates of both BWC and BKN fabrics are plotted in Fig. 4 and Fig. 5, respectively.

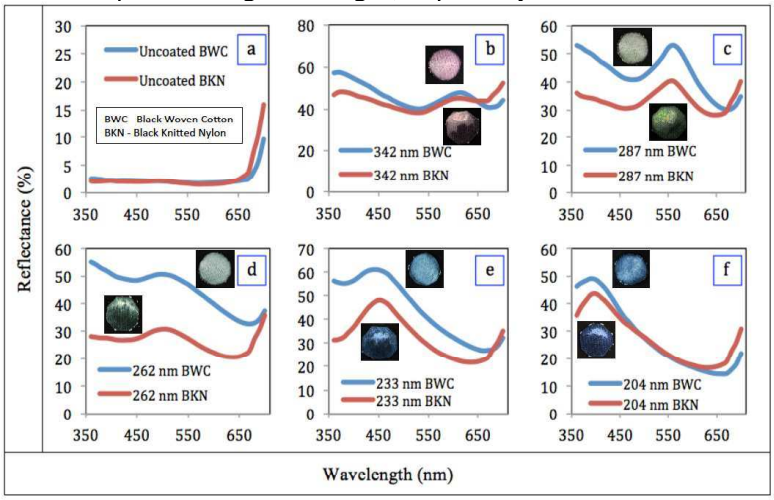

Fig. 4. Comparisons of the spectral reflectance of the uncoated (a) BWC and BKN fabrics, and those coated with 342 nm (b), 287 nm (c), 262 nm (d), 233 nm (e), and 204 nm (f), respectively.

The original uncoated BWC and BKN fabrics appear black as they have a low reflectance (< 3%) for the majority of the visible spectrum as shown in Fig. 4(a). Although the original BWC fabric has a higher reflectance beyond the wavelength of 650 nm, the value is still low (<15%) and suggests a peak value outside the visible range. However, the SNP-coated BWC and BKN fabrics show increased reflectance as shown in Fig. 4(b)-(f), and a peak wavelength can be observed for each coated fabric. Specifically, the smaller the SNP size the shorter peak wavelength that can be observed in the visible range, and this is in agreement with Bragg's law. In addition, it was found that the location of the peak may be determined by the SNP diameter regardless of the type of fabric. The BKN sample shows a generally lower reflectance than the BWC sample near to its peak wavelength, this is probably due to less coverage of the SNPs on the BKN fabric, resulting in a non-uniform and duller structural colour. Interestingly, some local areas of the SNP-coated BKN have a more intense colour than the BWC fabric treated with same sized SNP, especially the local bright yellow colour in Fig. 3(b) compared with the overall uniform duller colour in Fig. 1(b). This is probably due to the uneven surface of the knitted structure, which leads to a less uniform SNP coating. The intense colour arises from the SNP coating where the isolated thicker SNP ordered PC blocks are formed with insufficient surrounding disordered SNP arrangement.

It should be noted that there exist two peak wavelengths for each SNP-coated fabric, one in the visible range, and another in the ultraviolet range. As shown in Fig. 4(b), the two peaks are 370 nm and 610 nm for both SNP-coated fabrics, this is in good agreement with the data published by Yuan *et al.* [37] who measured the two peaks of 371 nm and 604 nm for a red coloured fibrous membrane consisting of randomly distributed colloidal crystal fibres. However, for the samples in Fig. 4(c)-(f), the peak in the ultraviolet range exceeds the spectral range of the spectrophotometer, and therefore cannot be detected. The higher peak in the visible range may be explained using Bragg's diffraction from the ordered SNP photonic crystal, while the lower peak is due to Mie scattering [37] and occurs due to the disordered SNP arrangement.

The CIE chromaticity coordinates x and y for both SNP-coated fabrics are plotted on the CIE 1931 2 degree Chromaticity Diagram, Fig. 5. The outer horse-shoe shaped boundary in Fig. 5(a) represents the spectral locus whose peak wavelength ranges from approximately 400 nm to 700 nm. The location of the chromaticity coordinates of the two sets of fabrics is located away from the spectral locus. This means that the structural colour of the fabrics is dull, with little saturation. The enlarged observation of the data in Fig. 5(b) shows that the uncoated fabric is surrounded by SNP-coated fabrics and the change of the chromaticity values with SNP diameter matches the order of the spectral locus regardless of the fabric types. As the SNP diameter decreases, the location of the chromaticity value changes from right to left, representing a blue-shift of the structural colours. This trend shows the positive correlation between the particle size and the observed structural colour, which has been previously explained using a modified Bragg's equation, Eq. 1.

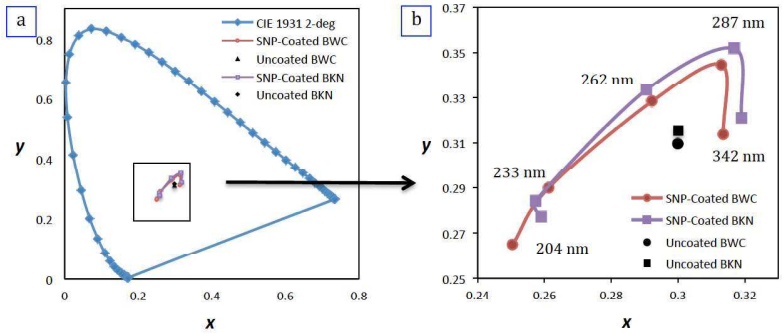

Fig. 5. CIE 1931 chromaticity values (a) for the uncoated and SNP-coated BWC and BKN fabrics; an enlarged plot of those values in (b) where the average diameter of the SNPs are displayed besides the relevant values.

3.3 Effect of fabric colour on the optical properties of SNP-coated fabrics

Although the structural colours produced on BKN fabrics were less uniform than those observed on BWC fabrics, those black fabrics have been successfully coloured using the SNPs, and the structural colours produced are tuned by SNP size. However, because most natural/synthetic fibres are originally white in colour, it is necessary to determine if the SNPs can colour a piece of white fabric using the sedimentation method.

Fig. 6(a)-(e) shows images of SNP-coated WKC fabrics with SNP diameters of 342 nm, 287 nm, 262 nm, 233 nm, and 204 nm, respectively. On visual inspection of the samples little difference in chroma could be perceived by the observer regardless of the applied particle size. The SNP-coated WKC fabrics appear to be a similar shade of white as the original WKC fabric. As can be seen from the SEM micrographs the SNPs did cover the surface. However, by analysing the SEM micrographs, it was observed that the SNP-coated WKC fabrics had a similar surface morphology to the BKN fabrics, with both ordered and disordered SNP arrangements being identified on the fabric surface. Fig. 6(f)-(h) show the surface SEM images of the WKC fabric coated with 233 nm diameter SNPs as shown in Fig. 6(c) at different magnifications. The fabric is covered by SNPs over a large area as shown in Fig. 6(f)-(g), both ordered and disordered SNP arrangement are observed as shown in Fig. 6(h). It can be assumed that a particular structural colour will still have been produced from such ordered photonic crystal structure due to Bragg's diffraction, but it is contained within a wider spectral range of reflection from the white fabric, resulting in the 'masking' of the structural colour to be perceived.

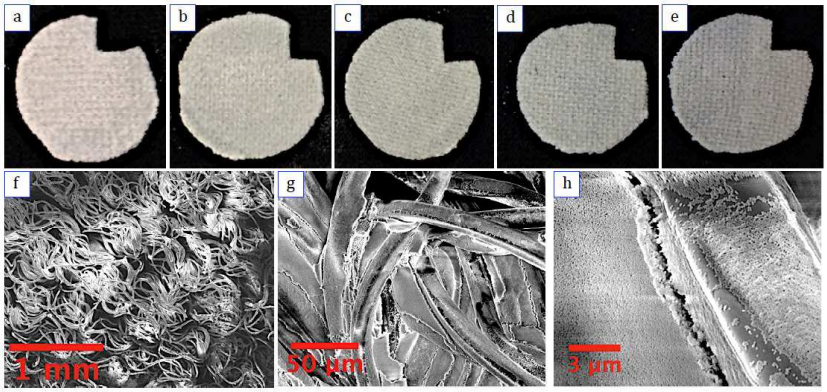

Fig. 6. Images of WKC fabrics coated with SNPs with average diameters of 342 nm, 287 nm, 262 nm, 233 nm, and 204 nm, from (a) to (e), respectively; the surface SEM images of (c) are given at different magnification of 25 (f), 400 (g), and 2.5K (h). The fabric diameter is approximately 25 mm. The top right section of each of the circular fabrics was cut to provide samples for SEM examination.

Table 1. The CIE *L, *a**, *b** values of original and SNP-coated WKC fabrics as shown in Fig. 6(a)-(e).**

SNP Diameter (nm)	Original	342	287	262	233	204
*L**	93.75	93.16	92.31	92.44	92.48	92.16
*a**	-0.42	-0.28	-1.14	-1.35	-1.46	-1.33
*b**	2.72	2.59	3.46	3.42	2.45	1.88
*C**	2.75	2.61	3.64	3.68	2.85	2.30
h°	98.78	96.17	108.24	111.54	120.79	125.28

In 1976 the CIE (Commission Internationale de l´Eclairage) specified the CIELAB colour space consisting of three values L*, a*, and b*. The lightness, *L**, are represented as the *z*-axis in the colour space, the *a* and b** values describe the degree of the colour in term of red (+a*) to green (-a*) and yellow (+b*) to blue (-b*), which are represented on the x and y-axis, respectively. Table 1 summarises the *L**, *a**, *and b** values of the original uncoated and SNP-

coated WKC fabrics with SNP diameters ranging from 342 nm to 204 nm, as shown in Fig. 6(a)-(e). The colour difference between the SNP-coated and original uncoated fabrics can be quantified using the general CIELAB colour difference formula recommended by the CIE in 1976, which is given in Eq. 2:

$$\Delta E^* = [(\Delta L^*)^2 + (\Delta a^*)^2 + (\Delta b^*)^2]^{1/2}, \quad (2)$$

where ΔE^* is the total colour difference, ΔL^* is the difference of lightness, Δa^* is the difference of a^* value, and Δb^* is the difference of b^* value. The total colour difference ΔE is calculated as 0.62, 1.77, 1.76, 1.67, and 2.01 for the five comparisons between each of the SNP-coated fabrics and the original fabric. Commercial tolerances of the colour difference are generally smaller than 2 [38], so the experimental colour measurements are in agreement with the visual observation of the colour difference of the fabrics.

In addition, the L^* values of the SNP-coated fabrics are smaller than the value of the original fabric. The reason for this could be the lower lightness value of the SNPs compared to the lightness value of original white fabric, as the SNPs covering almost the entire fabric's surface. The values of Δa^* and Δb^* for the five comparisons are plotted in a Cartesian coordinate system as shown in the Fig. 7(a). The origin of the system represents the standard sample, the original uncoated fabric in this case. The fabric coated with 342 nm SNP, it is located in the forth quadrant, which means that the coated fabric is redder/bluer compared to the original fabric. When the SNP diameter decreased to 287 nm and 262 nm, the location of the fabric moves to the second quadrant, and finally, the location moves to the third quadrant when the diameter further decreases to 233 nm and 204 nm. This trend indicates that the hue of the SNP-coated fabric will have small changes in the red, yellow, green, to blue directions when the SNP diameter decreases from 342 nm to 204 nm, although these changes will be difficult to visually detect for an observer. A similar trend is found in the chromaticity diagram as shown in Fig. 7(b). It can be seen that the location of the original uncoated fabric is surrounded by the SNP–coated fabrics, it proves the effect of the particle size to the structure colour of the fabric just as seen previously in Fig. 5 for the SNP-coated BWC and BKN fabrics.

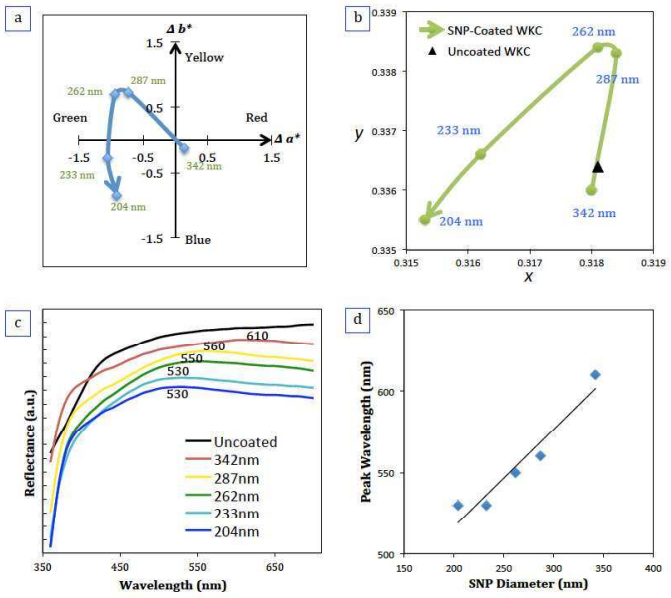

Fig. 7. The colour difference in terms of Δa^* and Δb^* between the SNP-coated and original WKC fabrics are plotted in a Cartesian coordinate system (a); CIE 1931 chromaticity values (b) and reflectance spectra (c) of the SNP-coated and original fabrics coated with SNPs having average diameters given in the figure legend; plot of the peak wavelength (d) of the SNP-coated fabrics against the average particle diameter. See **Data File 1** for all spectral values from (c).

Fig. 7(c) shows the spectral reflectance of each SNP-coated and uncoated WKC fabrics. All fabrics show high reflectance values (>70%) across the full visible spectrum, which is the reason why they all look white. It should be noted that the original white fabric (the black curve) does not have a peak wavelength in the visible range, however, a peak wavelength will appear when it is coated with SNPs. There still exists a positive correlation between the particle size and the peak wavelength, as shown in Fig. 7(d). In addition, the peak location for the WKC fabrics coated with 342 nm and 287 nm-sized SNP are exactly the same as the BWC and BKN fabrics, which are 610 nm and 560 nm, respectively. This indicates the photonic crystal structure has been formed on the WKC fabric just as seen on the BWC and BKN fabrics although the structural colour from such ordered structure on the white fabric is difficult to detect for an observer.

4. Conclusions

Silica photonic crystals have been formed on flexible textile fabrics by the self-assembly of SNPs using the gravitational sedimentation technique. The optical properties of the SNP-coated fabrics are affected by the silica particle size, fabric structure, and fabric background colour. Specifically, uniform and non-iridescent structural colours have been produced on the tight black woven cotton fabric. The overall colour effect is produced by the combination of Bragg's diffraction from the ordered photonic crystals and the Mie scattering from the disordered SNP arrangement. The structural colour is SNP size-dependent, the larger the particle size the longer the peak wavelength of the colour obtained. When using a black knitted nylon fabric, the size-dependent structural colour is also produced but less uniform due to the large yarn spacing. However, if the original fabric is white in colour, the SNP-coating produced little perceivable structural colour on visual inspection due to the strong light reflection from the original white fabric and the Mie scattering from the disordered SNP arrangement. However, the SEM examination revealed that the ordered photonic crystal structure was also produced on the white fabric, and the instrumental colour measurements show that there still exists a positive correlation between the peak wavelength and the particle size. This work reports the optical properties of textile substrates coated with silica nanoparticles, and investigates factors that influence the quality of the structural colours produced.

Funding

Society of Dyers and Colourists (SDC) Main Bursary (July 2014).